Light scattering and downstream applications with high-performance computing capabilities

Ping Yang, Masanori Saito, Jiachen Ding, Tong Ren, Yi Wang, Adam Bell,
Boyan Gu, James Coy, and Jeffrey Mast
Department of Atmospheric Sciences, Texas A&M University

Remote Sensing Development

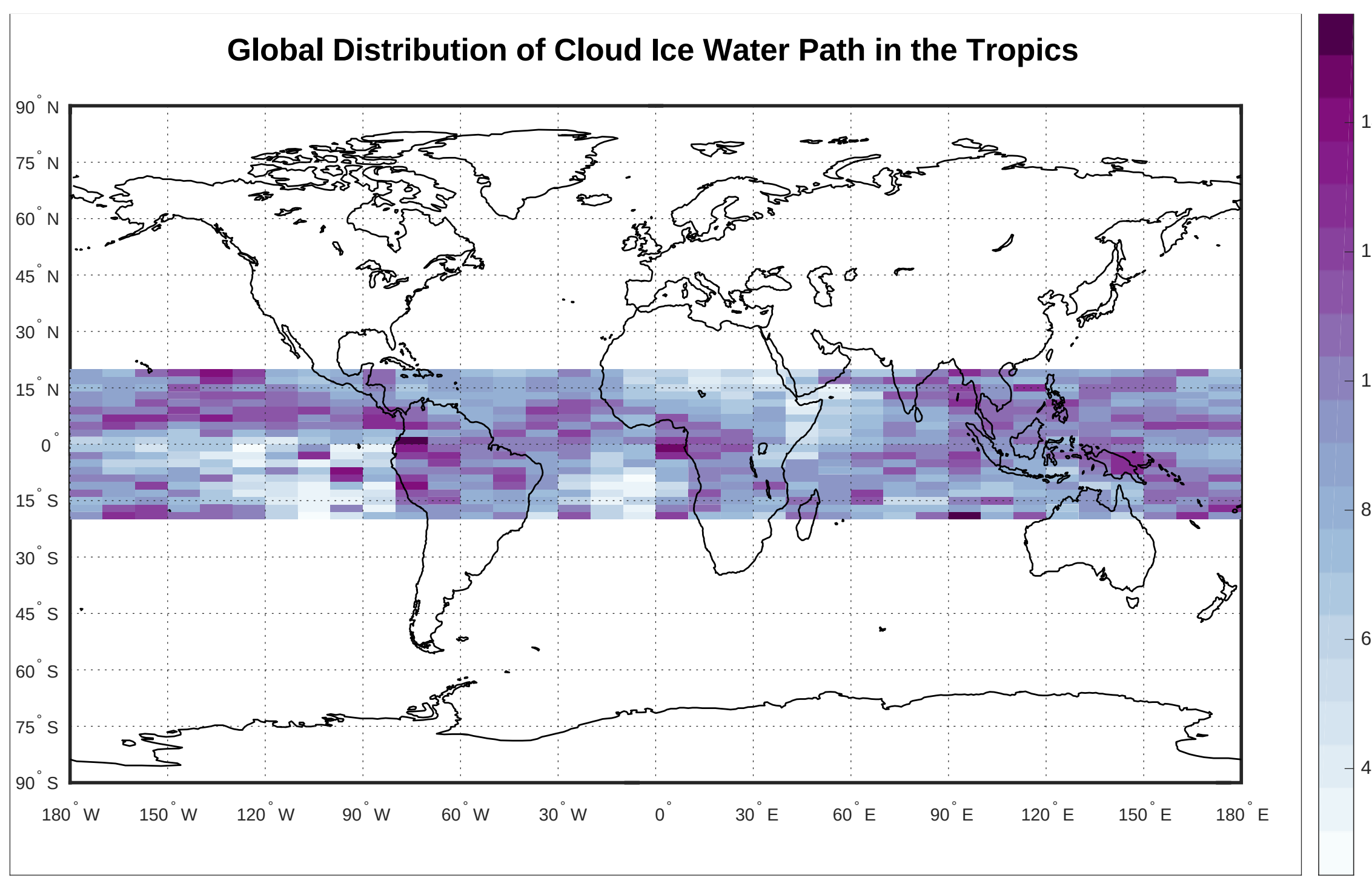

Fig. 4. Global distribution of cloud ice water path in the Tropics.

There are discrepancies in the magnitude of cloud ice among many current global climate models. To mitigate this, global measurements of cloud ice are needed. This figure shows the global distribution of cloud ice mass. One year of satellite data from CloudSat is used to generate synthetic measurements, and ice water path is then inferred from those measurements using a new retrieval methodology.

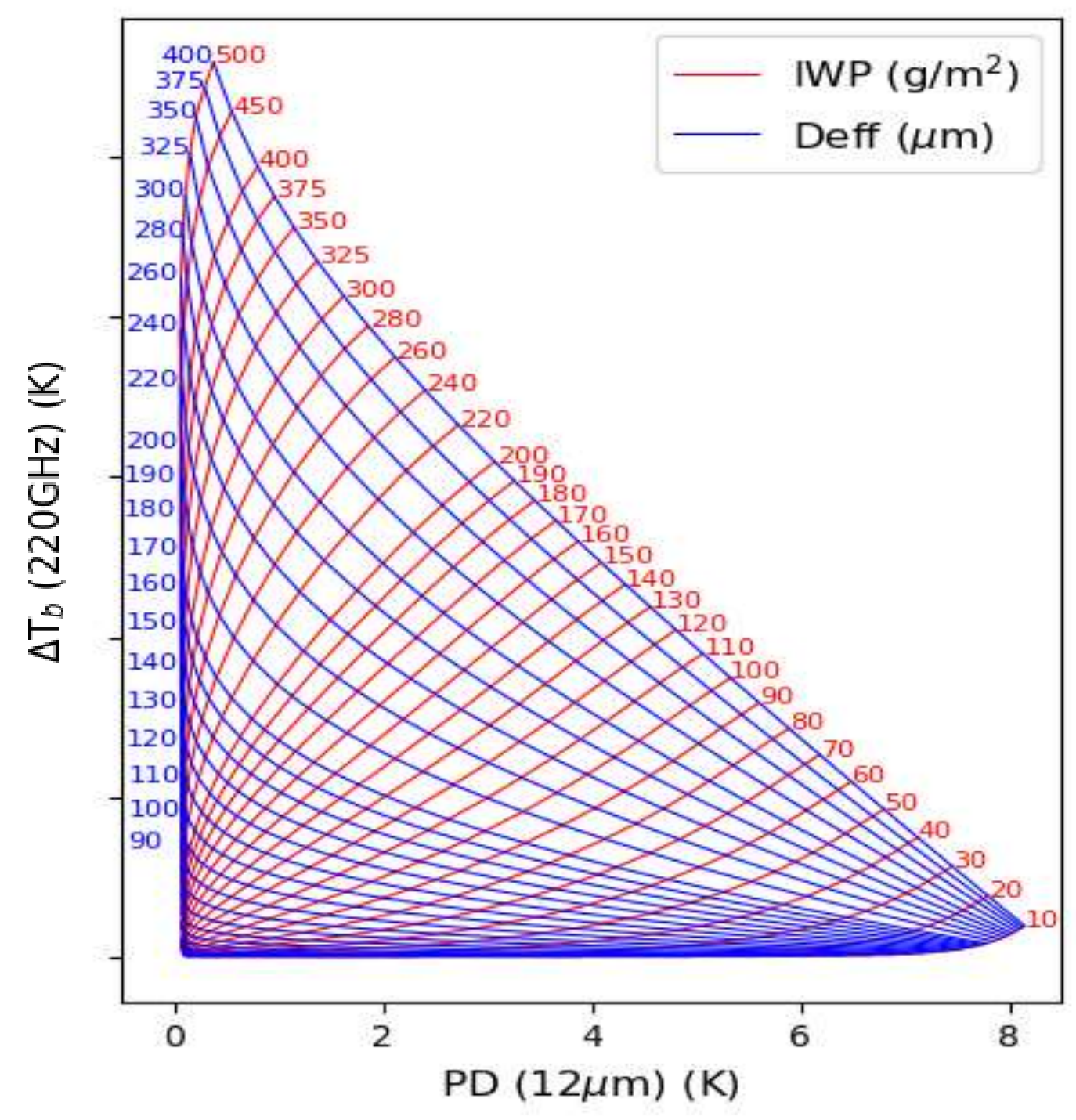

Fig. 5. A lookup table diagram for ice cloud IWP and D_{eff} retrievals using passive microwave (220 GHz) and thermal infrared ($12\mu m$) measurements.

Ice Water Path (IWP) and Effective Diameter () isoline Lookup Table with respect to 12µm polarization difference (PD) and 220GHz brightness temperature depression from clear-sky (). Calculated from Atmospheric Radiative Transfer Simulator (ARTS) program with the goal of utilizing polarized microwave and infrared wavelengths to infer ice cloud properties.

Optical Phenomenon Simulation

Fig. 6. Optical phenomena simulations: (Left) Parhelia, and (right) upper tangent arc.

Horizontally oriented ice crystals in the atmosphere cause particular optical phenomena such as Parhelia and the upper tangent arc. These optimal phenomena are simulated based on light scattering properties (Saito and Yang, 2019).

RTM Development

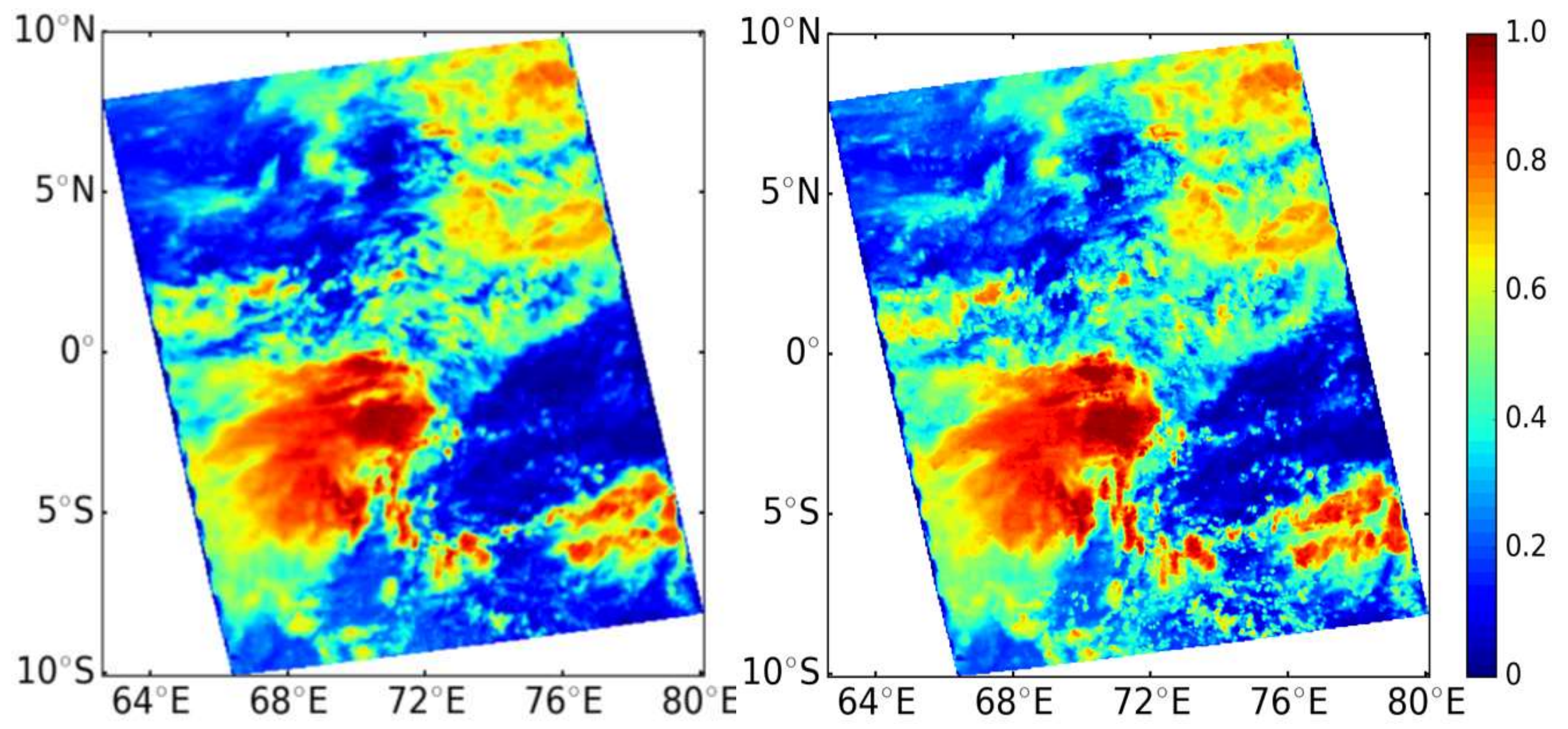

Fig. 7. Observed (left) and simulated (right) Polarization and Directionality of the Earth's Reflectances (POLDER) radiometer reflectance at 0.865 µm band.

The simulation is performed by TAMU Vector Radiative Transfer Model (TAMU-VRTM) (Ding et al. 2019).

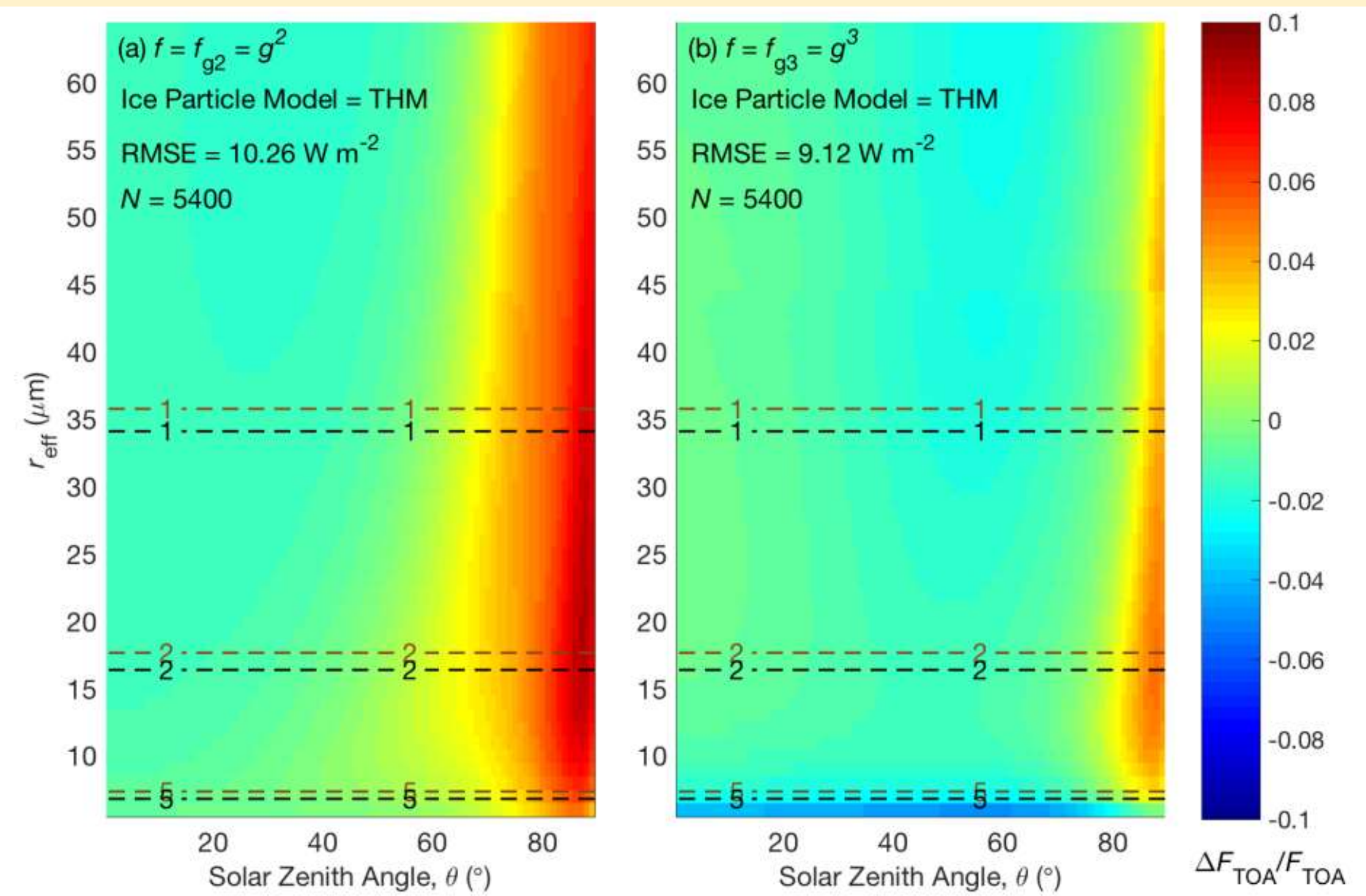

Fig. 8. Shortwave flux biases at the top of atmosphere

The cube of asymmetry factor is a better parameterization of the fraction of forward scattering than the conventional approach in the two-stream approximation in terms of the shortwave broadband radiation flux calculations at the top of the atmosphere and the surface.

Light scattering simulations

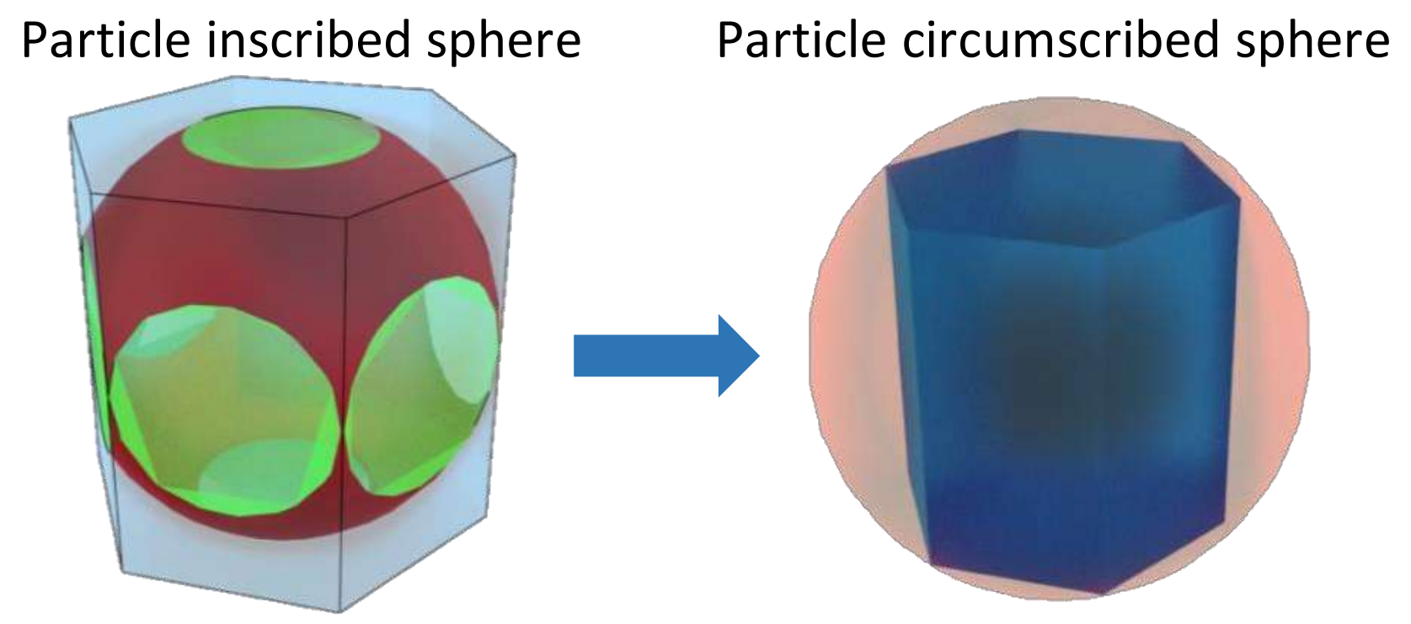

Fig. 1. Invariant Imbedding T-matrix Method (II-TM)

II-TM is used for particles with small-to-moderate sizes.

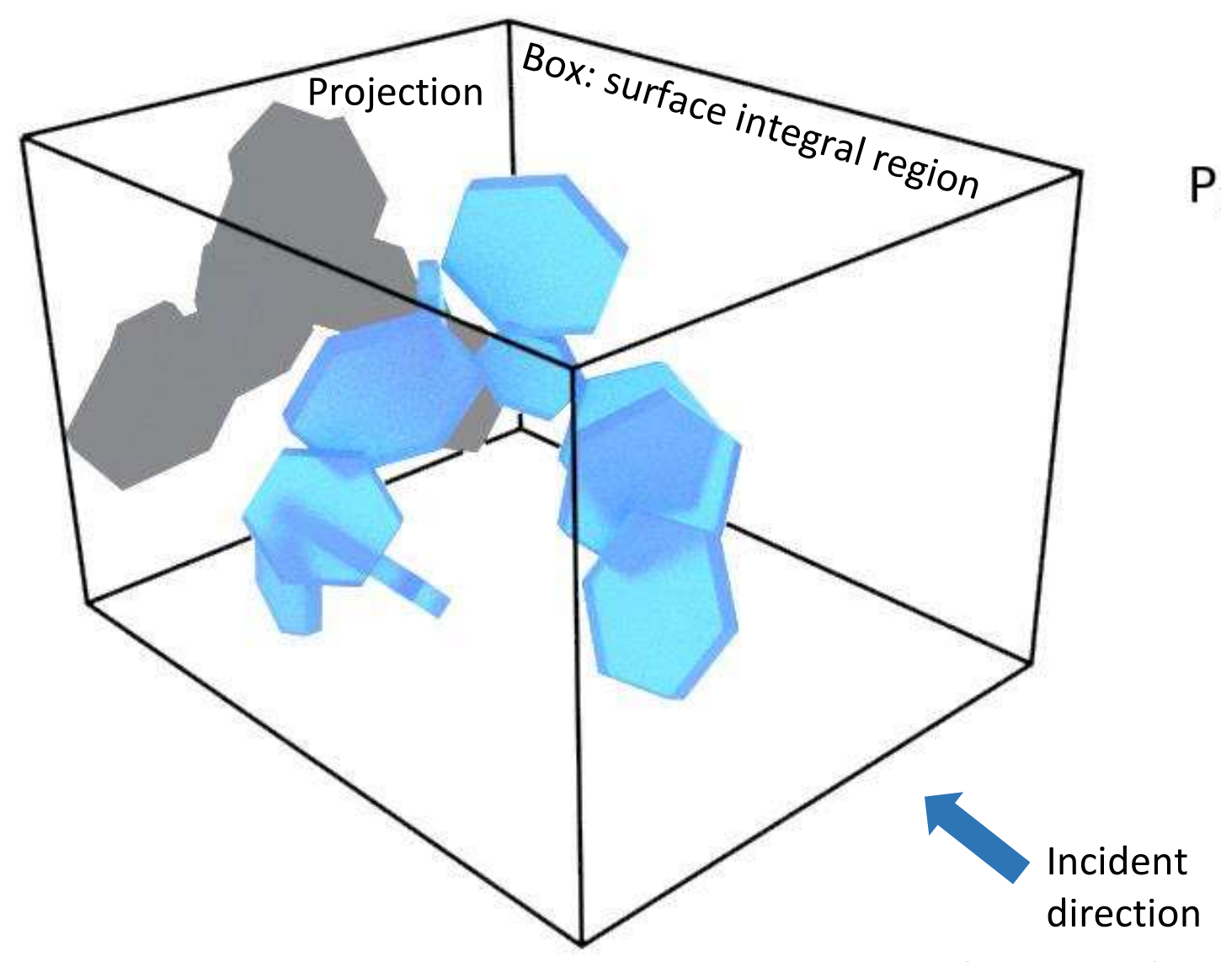

Fig. 2. Physical Geometric Optics Method (PGOM)

PGOM is used for particles with moderate-to-large sizes.

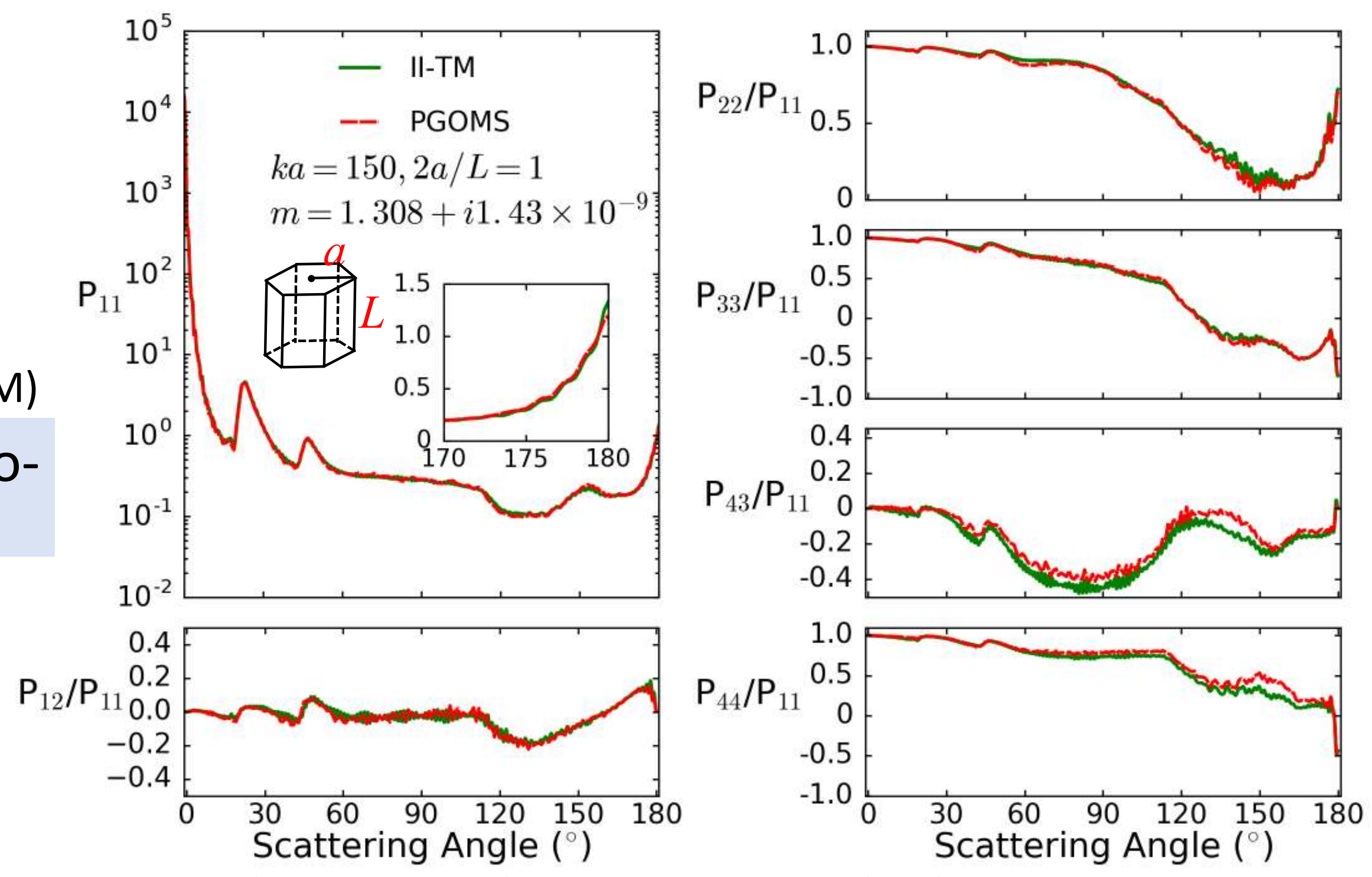

Fig. 3. Phase matrix elements computed by the II-TM and PGOM.

Light scattering calculations require large computational expense (Yang et al. 2019). Single-scattering property database are widely used in research communities and are developed with the Texas A&M University Supercomputing Facilities.

Satellite Data Analysis

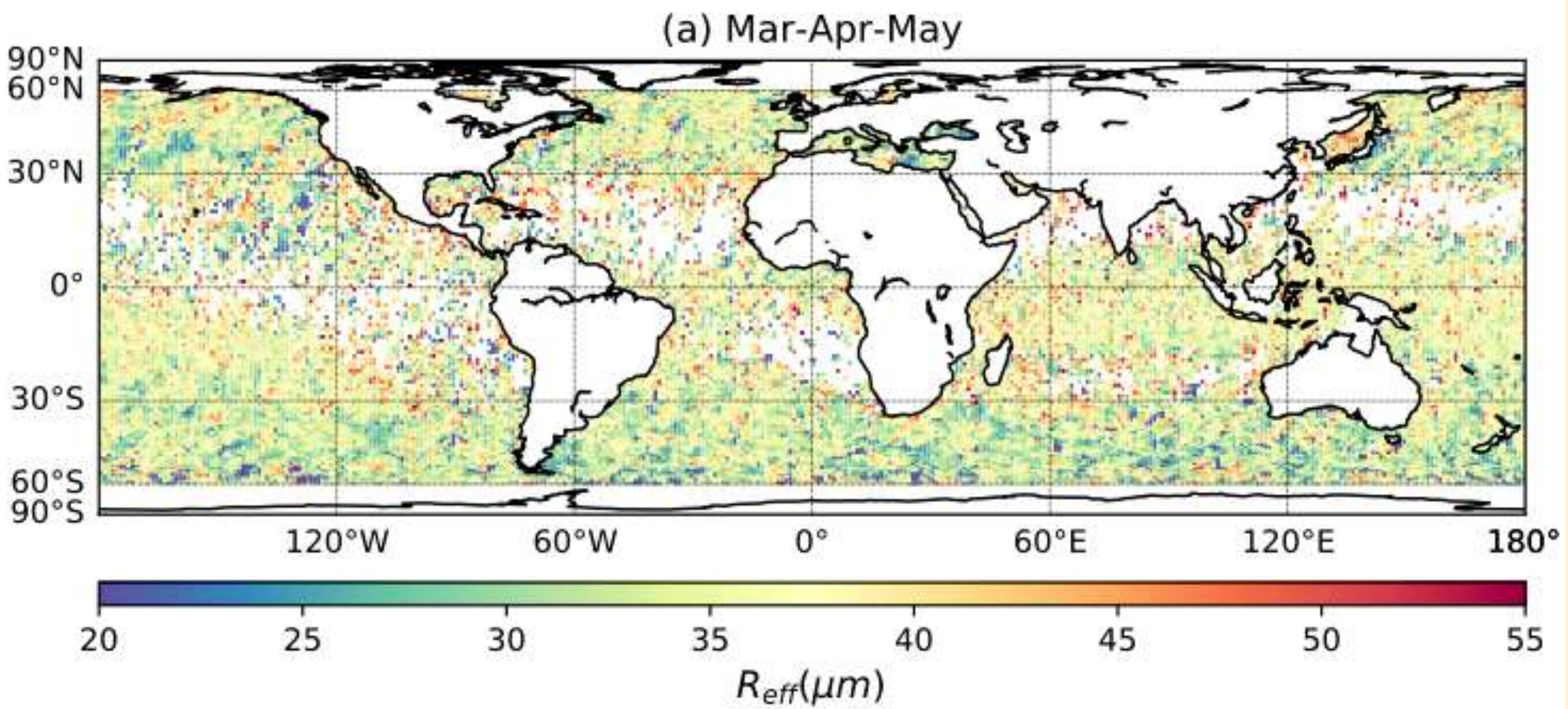

Fig. 10. The global distribution of ice cloud effective radius.

Global distribution of effective particle radius of ice clouds in 2013 assuming optimal ice particle model (Wang et al. 2018) retrieved from multi-angle imaging satellite measurements (NASA Terra MISR).
Data size: 5.5 TB
CPU core: 1000
Around 150 hours/core

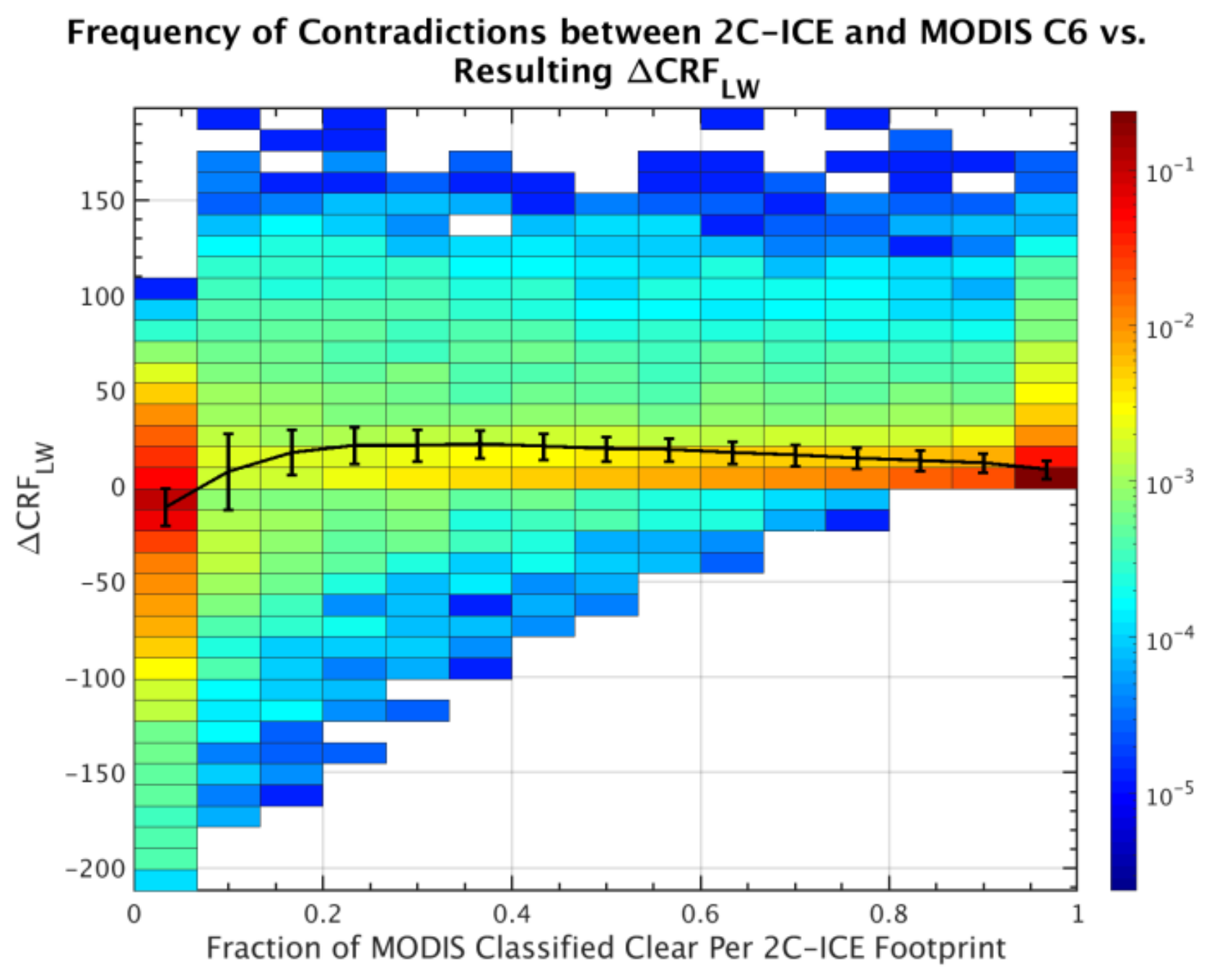

Fig. 11. Cloud radiative forcing bias among satellite cloud products.

It is known that ice cloud retrievals that are based on passive sensors misclassify scenes with very optically thin cirrus clouds as clear sky. We show that cloud radiative forcings calculated using MODIS C6 products have an apparent bias when compared to similar calculations using a collocated active sensor retrieval (2C-ICE) for such scenes. This bias, due to very optically thin ice clouds, is approximately 8 W/m².

Global Energy Budget

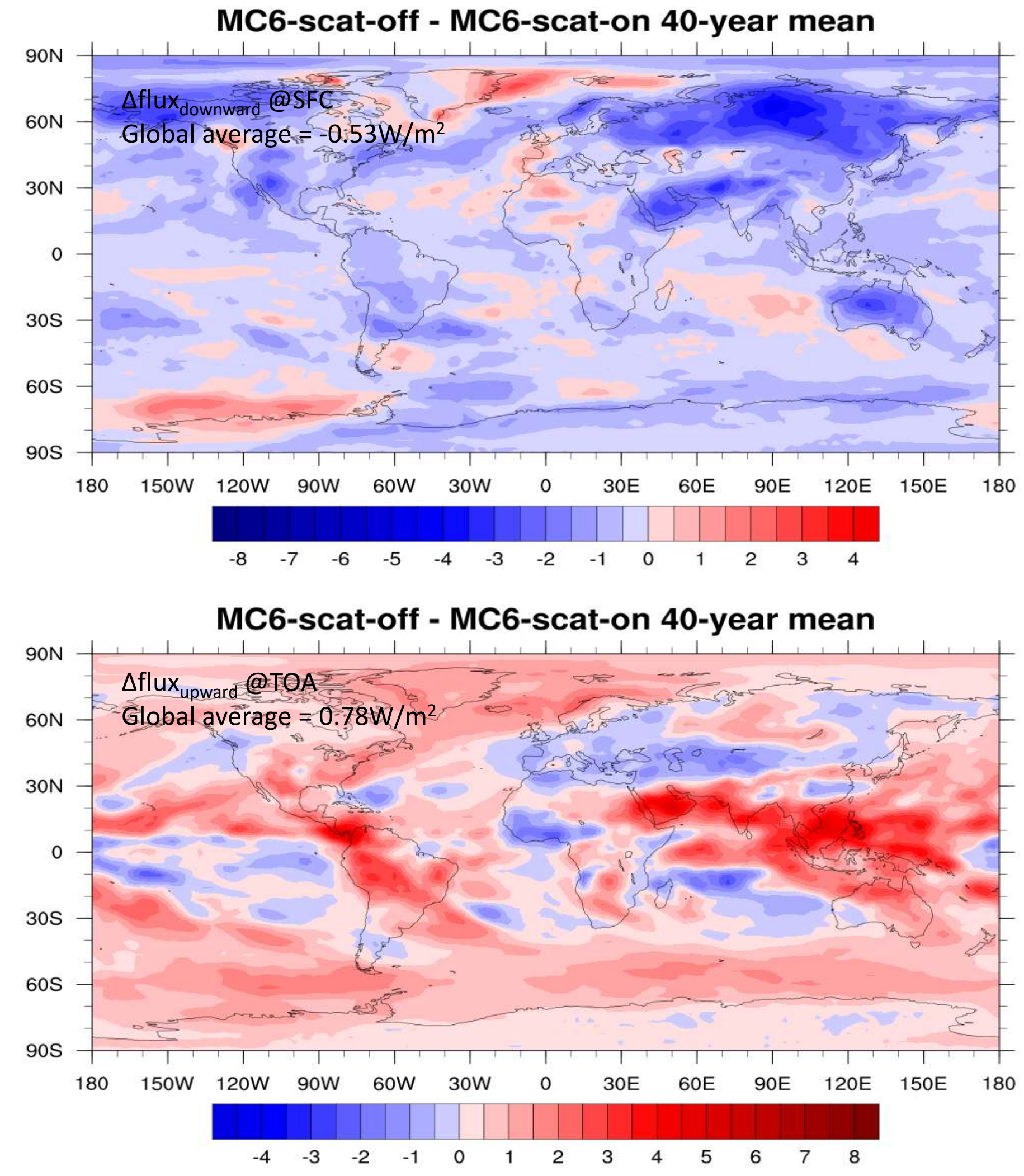

Fig. 9. The global distribution of 40-year mean surface downward flux difference and the TOA upward flux difference between with or without longwave cloud multiple scattering using MODIS Collection 6 cloud optical properties.

The global averaged LW surface downward flux is underestimated by about 0.53W/m², while the global averaged LW TOA flux is overestimated by about 0.78W/m², if scattering is neglected in the CESM simulations.

References

1. Ding et al. (2019), *J. Quant. Spectrosc. Radiat. Transfer*, 106667.
2. Saito and Yang (2019), *J. Atmos. Sci.*, **47,** 1878–1893.
3. Yang et al. (2019), Prog. In Electro. Res., **164,** 27–61.
4. Wang et al. (2018), *Remote Sens.*, **10,** 51–69.